Chapter 7

A Novel Idea of Coherent Acoustic Wave-Induced Atmospheric Refractivity Fluctuation and Its Applications

Shuhong Gong, Yu Liu, Muyu Hou and Lixin Guo

Additional information is available at the end of the chapter

http://dx.doi.org/10.5772/intechopen.70996

Abstract

The physical mechanism of generating the lasting tropospheric refractivity fluctuation with a stable array-distributed structure by coherent acoustic waves is investigated. An example of the quantitative calculation of atmospheric refractive index is given and analyzed. Based on the theory of electromagnetic wave propagation and scattering in the troposphere, the feasibility to purposefully affect radio wave propagation is qualitatively demonstrated by the experiment of the coherent acoustic source-induced laser interference fringe change. The potential application aspects of synthetically controlling the radio wave propagation by the artificial refractivity fluctuation structure are preliminarily proposed. This chapter will promote the development of the coherent acoustic wave-induced tropospheric refractivity fluctuation, and it has the important theoretical significance and potential application value to purposely apply the positive or negative effects on radio wave propagation.

Keywords: troposphere, atmospheric refractive index, coherent acoustic waves radio wave propagation, positive or negative effects

1. Introduction

Radio wave propagation is an important part of wireless systems. The investigations into various environment channel media with different physical properties, different dielectric properties, and spatiotemporal structures are inevitable to research radio wave propagation. There are two types of influences induced by the environment media on the radio wave propagation: the one is to realize particular propagation mode and advanced wireless technology, such as to realize the over-the-horizon communication or detection by atmospheric

turbulence scattering and the multiple-input multiple-output wireless system by multipath propagation, which is seen as the positive influence; the other is to restrict radio signal propagation to be received or detected. For instance, the propagation effects of attenuation, depolarization, scintillation, and atmospheric noise are restrictive effects on communication systems, which are seen as the negative influence. It is the goal of the research on radio wave propagation to investigate the propagation environment media-caused positive influence and negative one and to apply them to the two aspects, based on the precondition of sufficiently mastering and controlling the physical and dielectric properties of propagation environment media. On the one hand, it makes the performances of an expected wireless electronic system perfectly match with its wireless channel, by forecasting, modifying, and applying the positive effects. On the other hand, it destroys the original perfect match between the hostile wireless electronic system and its wireless channel during wireless system countermeasures, by forecasting, creating, and controlling the negative effects.

The idea of coherent acoustic wave-induced atmospheric refractivity fluctuation is to control the characteristic parameters of radio wave, such as amplitude, phase, propagation direction, and polarization, by the propagation effects caused by the artificial atmospheric refractivity fluctuation. And, the final aim is to purposefully apply the positive effects or the negative effects. Note that the idea of coherent acoustic wave-induced atmospheric refractivity fluctuation and its application is a new field and is in its infant stage.

The idea of changing the tropospheric refractivity by the disturbance of acoustic wave is first proposed in [1], in which A. Tonning pointed out the viewpoint that an acoustic wave propagating in the troposphere can cause the atmospheric refractivity fluctuation and theoretically analyzed the rationality of the viewpoint. In the next 50 years, radio acoustic sounding system (RASS) began to be established to detect atmospheric temperature, wind profile, and turbulence in the lower troposphere [2–4]. The first RASS system to measure atmospheric temperature profile was born at Stanford University [5]. By the 1990s, this technique was adopted to solve the problems of measuring the temperature in indoor environment [6–9], also employed to detect the wake vortex of aircrafts [10, 11], and even explored to track and detect the taggant for the soldier identification friend-or-foe application [12]. Currently, RASS can detect the atmospheric parameters below 20 km [13]. The RASS history was summarized, and the applications of RASS in the detection of turbulence were analyzed in [14]. The applications and limitations of RASS system are analyzed in [15]. Afterward, the broadband acoustic pulse technology [16] and imaging techniques [17] are applied to RASS system.

The idea of coherent acoustic wave-induced tropospheric refractivity fluctuation mentioned in this chapter is fundamentally different from RASS. The main idea of RASS is to obtain the parameters of atmospheric physical properties based on the relationship between acoustic propagation velocity and atmospheric physical property parameters by tracking the velocity of acoustic wave front which can be seen as an artificial refractivity irregularity. However, the main idea, in this chapter, is to purposely apply the positive influences and negative ones induced by artificial array-distributed refractivity irregularity, which is stable, lasting, and controllable because the coherent acoustic source is used. The viewpoint to purposely affect radio wave propagation by a coherent acoustic source is proposed for the first time in [18]. In this

chapter, the physical mechanism of generating the lasting tropospheric refractivity fluctuation with stable array-distributed structure by coherent acoustic waves is elaborated in Section 2, the distribution of the artificial atmospheric refractive index is quantitatively calculated, and the feasibility to purposefully affect radio wave propagation is qualitatively demonstrated by the experiment of the coherent acoustic source-induced laser interference fringe change in Section 3. The potential application aspects of synthetically controlling the radio wave propagation by the artificial refractivity fluctuation structure are preliminarily proposed in Section 4; further investigations in the future are listed in Section 5. This chapter will promote the development of the coherent acoustic wave-induced tropospheric refractivity fluctuation.

2. The mechanism of controlling the atmospheric refractivity fluctuation by coherent acoustic waves

The real part N of the atmospheric refraction index in the radio band is nearly independent of frequency. N depends on the atmospheric pressure P in hPa, the absolute temperature T in K, and the water vapor pressure e in hPa, and the relation among them is [19]

$$N = 77.6\frac{P}{T} + 373256\frac{e}{T^2} \tag{1}$$

Operating the difference algorithm on Eq. (1), the relation among ΔN, ΔT, ΔP, and Δe is given as

$$\Delta N = -\left[77.6PT^{-2} + 746512eT^{-3}\right]\Delta T + \left(373265eT^{-2}\right)\Delta e + \left(77.6T^{-1}\right)\Delta P \tag{2}$$

Eq. (2) shows that ΔN is closely related to ΔT, ΔP, and Δe. The refractivity fluctuation ΔN can be steered by controlling one or more parameters among ΔT, ΔP, and Δe according to Eq. (2).

Acoustic wave movement follows the three basic laws: Newton's second law of motion, law of conservation of mass, and thermodynamic equation of state [20]. The wave function of an acoustic wave can be derived from the three basic laws and is written as [21]

$$\nabla^2 p = \frac{1}{c_0}\frac{\partial^2 p}{\partial t^2} \tag{3}$$

where p is the instantaneous acoustic pressure and c_0 denotes the acoustic propagation velocity in the atmosphere. p and c_0 can be expressed as

$$p = \Delta P = P - P_0 \tag{4}$$

$$c_0 = 331.6 + 0.6t_t \tag{5}$$

In Eq. (4), P_0 and P are the atmospheric pressure in Pa before and after the disturbance by an acoustic wave, respectively. And t_t in Eq. (5) is the atmospheric temperature in °C. Eq. (3) shows that when an acoustic wave passes through the atmospheric medium, the additional periodical variational pressure, that is, acoustic pressure $p = \Delta P$, will be exerted upon the

medium based on the original atmospheric pressure. It is rational to neglect the temperature change induced by the additional periodical variational pressure; therefore $\Delta T = 0$. According to [18], ΔP and Δe satisfy the formula $\Delta e/e = \Delta P/P$. Therefore, Eq. (2) can be deduced as

$$\Delta N = \left(77.6T^{-1} + 373265e^2T^{-2}P^{-1}\right) \cdot p \tag{6}$$

It is shown in Eq. (6) that the refractivity fluctuation ΔN will present a specific spatial and temporal distributions along with the acoustic pressure p.

The solutions to Eq. (3) for the cases of the plane wave, the cylindrical wave, and the spherical wave can be, respectively, formulated as

$$p = p_A e^{j\left(\omega t - kr_p\right)} \tag{7}$$

$$p = \frac{p_A}{\sqrt{r_c - l_0}} e^{j[\omega t - k(r_c - l_0)]} \tag{8}$$

$$p = \frac{p_A}{r_s - r_0} e^{j[\omega t - k(r_s - r_0)]} \tag{9}$$

In Eqs. (7) and (9), p denotes the instantaneous value of the acoustic pressure at a point in their acoustic pressure field, r_p represents the distance between a planar acoustic source to a point in the acoustic pressure field, r_s represents the distance between the center axis of a cylinder-surface acoustic source to a point in the acoustic pressure field, r_0 represents the distance between the center of a spherical-surface acoustic source and a point in the acoustic pressure field, r_c is the diameter of the spherical-surface acoustic source, l_0 is the length of the cylindrical-surface acoustic source, and p_A is the acoustic pressure on the surface of the above acoustic sources. ω and k denote the angular frequency and wave number of the acoustic waves, respectively.

p_A for the three types of acoustic sources mentioned above can be, respectively, expressed as

$$p_A = \begin{cases} \left[2W\rho_0 c_0 S^{-1}\right]^{1/2} & \text{For plane acoustic source} \\ \left[2W\rho_0 c_0 (2\pi r_0 l_0)^{-1}\right]^{1/2} & \text{For cylindrical-surface acoustic source} \\ \left[2W\rho_0 c_0 \left(4\pi r_0^2\right)^{-1}\right]^{1/2} & \text{For spherical-surface acoustic source} \end{cases} \tag{10}$$

where W is the acoustic wave power radiated by the acoustic sources, S is the area of the plane acoustic source, and ρ_0 is the density of air.

In other words, when a spherical-surface acoustic wave passes through the homogeneous atmosphere medium, the distribution of acoustic pressure p or atmospheric refractivity fluctuation ΔN at a certain moment in a plane including the point acoustic source shown in **Figure 1** is similar to the waveform of a mechanical wave in water surface shown in **Figure 2**. Correspondingly, the refractivity fluctuation ΔN will present a similar spatial distribution following

http://dx.doi.org/10.5772/intechopen.70996

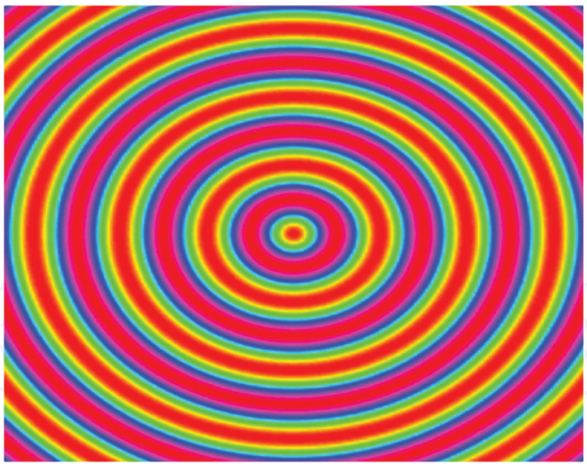

Figure 1. The spatial distribution of p or ΔN when a spherical-surface acoustic wave travel through the homogeneous medium.

Figure 2. The waveform of a water surface wave caused by a single source.

Eq. (6). It is by means of the reflection effect of the acoustic wave front with ΔN that the purpose of tracking the propagation speed of acoustic wave is realized in RASS.

The principle of independent propagation and superposition of waves indicates that if two coherent waves meet, the interference phenomenon can be formed. **Figure 3** shows the waveform when two coherent water surface waves meet. **Figure 4** shows the simulation of the distribution of p or ΔN when two coherent acoustic waves meet.

According to the wave interference theory, interference pattern is closely related to coherent wave frequency, phase, acoustic source structure, and so on. For any type of coherent acoustic source with array structure, the acoustic pressure at point $\vec{r}$ in the interference area can be expressed as

Figure 3. The waveform when two coherent water surface waves meet.

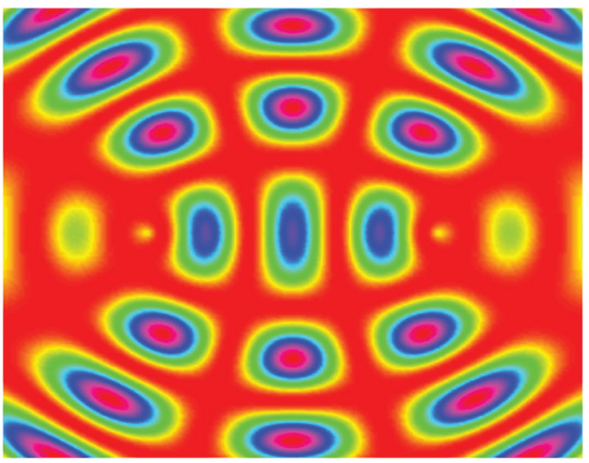

Figure 4. The distribution of p or ΔN when two coherent acoustic waves meet.

$$p\left(\vec{r}\right) = p_0\left(\vec{r}\right)|S| \tag{11}$$

where $p_0\left(\vec{r}\right)$ gives the acoustic pressure of single elements of the acoustic source array and $|S|$ is the array factor, which presents the interference process. The array factor of the uniform spherical-surface acoustic source planar array shown in **Figure 5** and the uniform cylindrical-surface acoustic source linear array shown in **Figure 6** are, respectively, given as [18]

$$|S(\theta,\phi)| = \left| \frac{\sin\left[N_x \frac{\pi b_x \sin\theta\cos\phi}{\lambda} + \beta_x\right]}{\sin\left[\frac{\pi b_x \sin\theta\cos\phi}{\lambda} + \beta_x\right]} \cdot \frac{\sin\left[N_y \frac{\pi b_y \sin\theta\sin\phi}{\lambda} + \beta_y\right]}{\sin\left[\frac{\pi b_y \sin\theta\sin\phi}{\lambda} + \beta_y\right]} \right| \tag{12}$$

http://dx.doi.org/10.5772/intechopen.70996

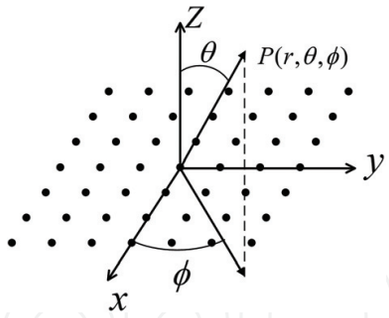

Figure 5. The sketch of a uniform spherical-surface acoustic source planar array.

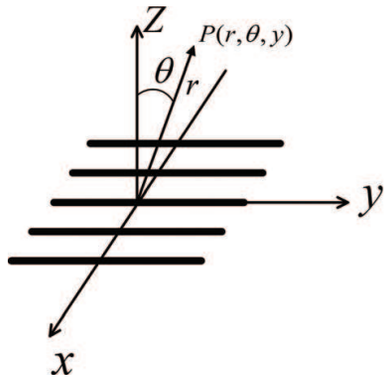

Figure 6. The sketch of a uniform cylinder-surface acoustic source linear array.

$$|S(\theta)| = \left| \frac{\sin\left[N\frac{b\sin\theta}{\lambda} + \beta\right]}{\sin\left[\frac{b\sin\theta}{\lambda} + \beta\right]} \right| \tag{13}$$

In Eq. (12), N_x and N_y are, respectively, the number of array elements along the x-axis and y-axis, and b_x and b_y are, respectively, the inter-element spacing along the x- and y-axes in **Figure 5**. In Eq. (13), N and b denote, respectively, the element number and the interval in **Figure 6**. λ is the acoustic wavelength. β_x and β_y are the harmonic vibration phase differences between the adjacent elements along x-axis and y-axis in **Figure 5**, respectively. β is the harmonic vibration phase difference between the adjacent elements in **Figure 6**. **Figures 7** and **8** are the simulating examples according to Eq. (12) and Eq. (13).

Therefore, the lasting artificial atmospheric refractivity irregularities with a stable, controllable, and subtle array structure in a specific space can be generated by setting the geometric structure of acoustic source and adjusting the frequency, amplitude, and phrase of acoustic waves. In [18], the coherent acoustic source shown in **Figure 9** and the short scattering communication link shown in **Figure 10** are used in the experiment. The experimental results as shown in **Figures 11–18** are observed, which further verify the feasibility of perturbation in the tropospheric atmospheric refractivity by coherent acoustic wave.

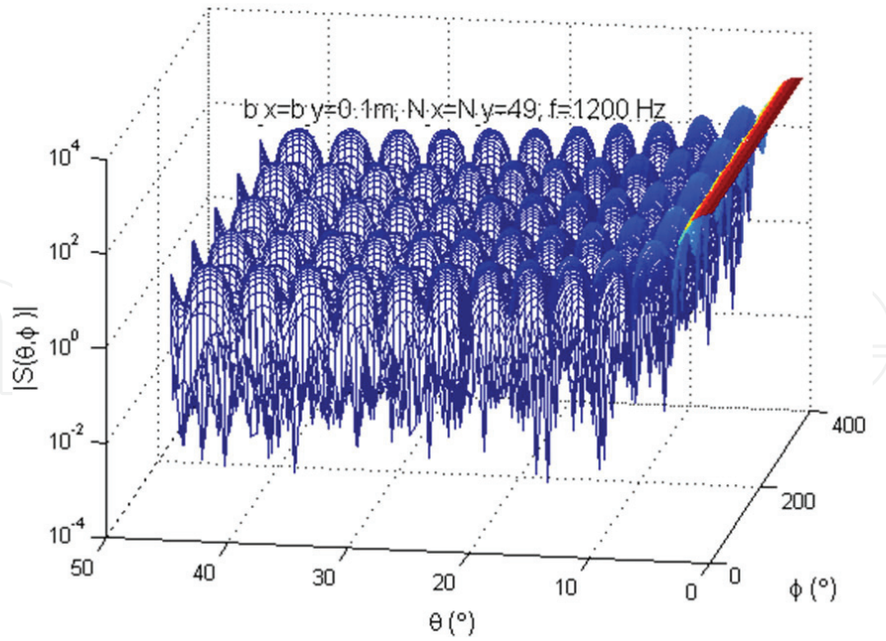

Figure 7. The simulation example of the array factor of the acoustic antenna array in **Figure 5.**

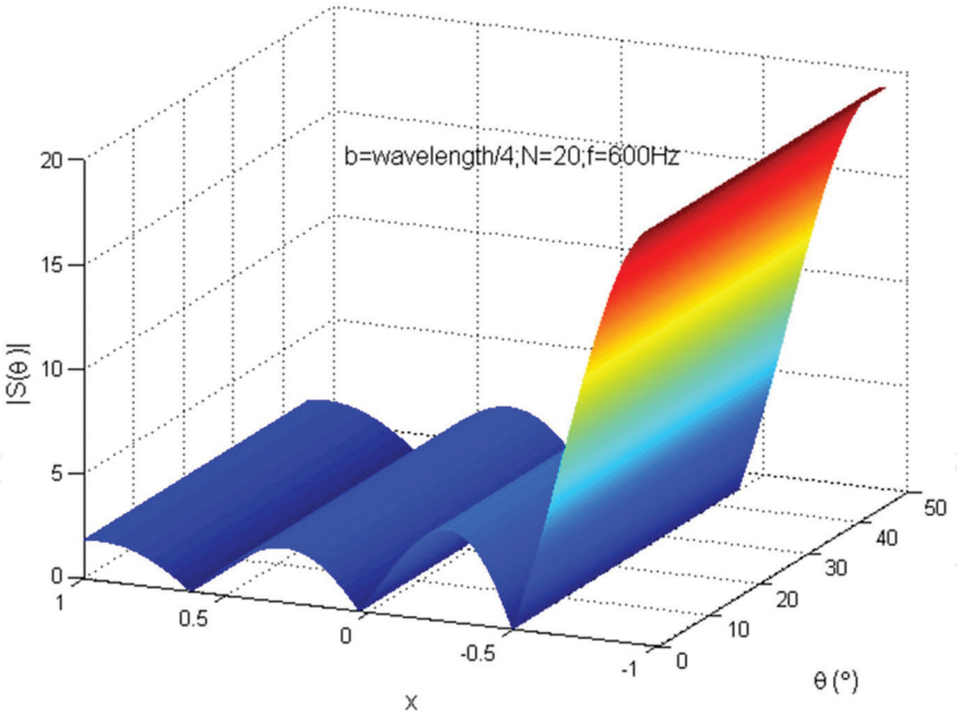

Figure 8. The simulation example of the array factor of the acoustic antenna array in **Figure 6.**

http://dx.doi.org/10.5772/intechopen.70996

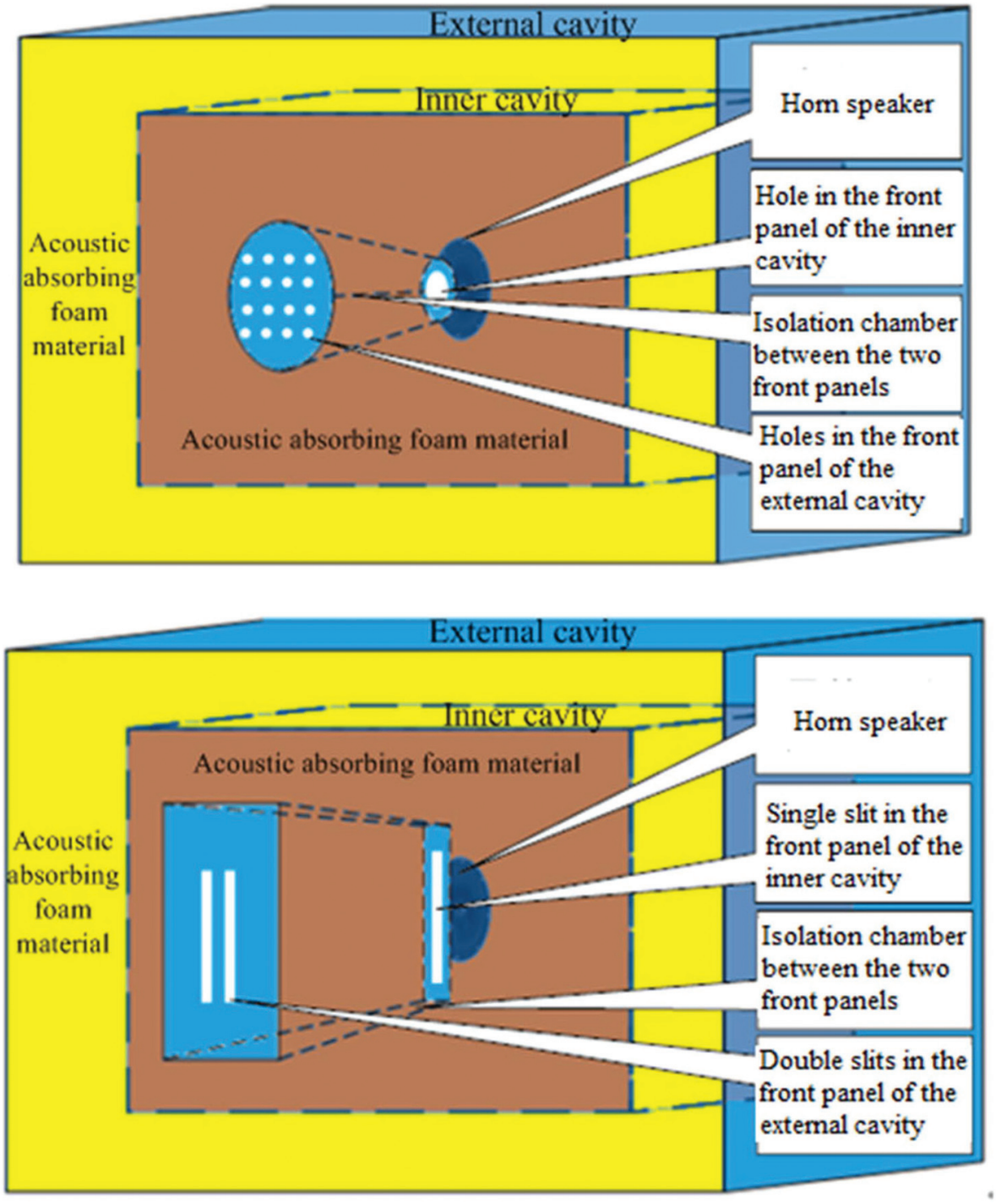

Figure 9. The sketch of the coherent acoustic source adopted in [18].

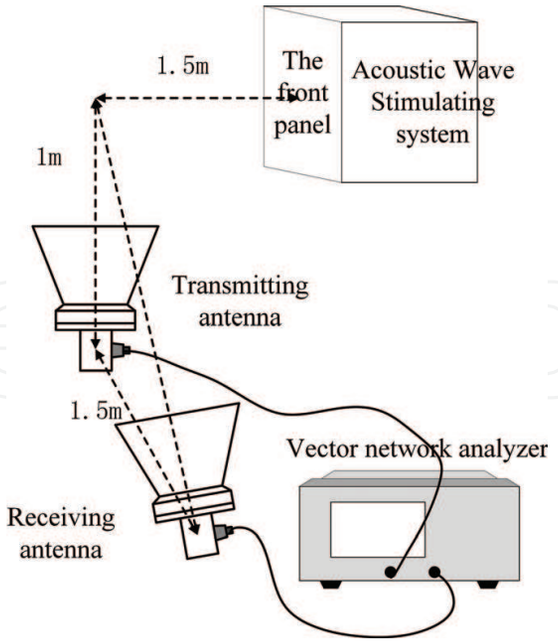

Figure 10. The sketch of the radio link adopted in the testing experiment in [18].

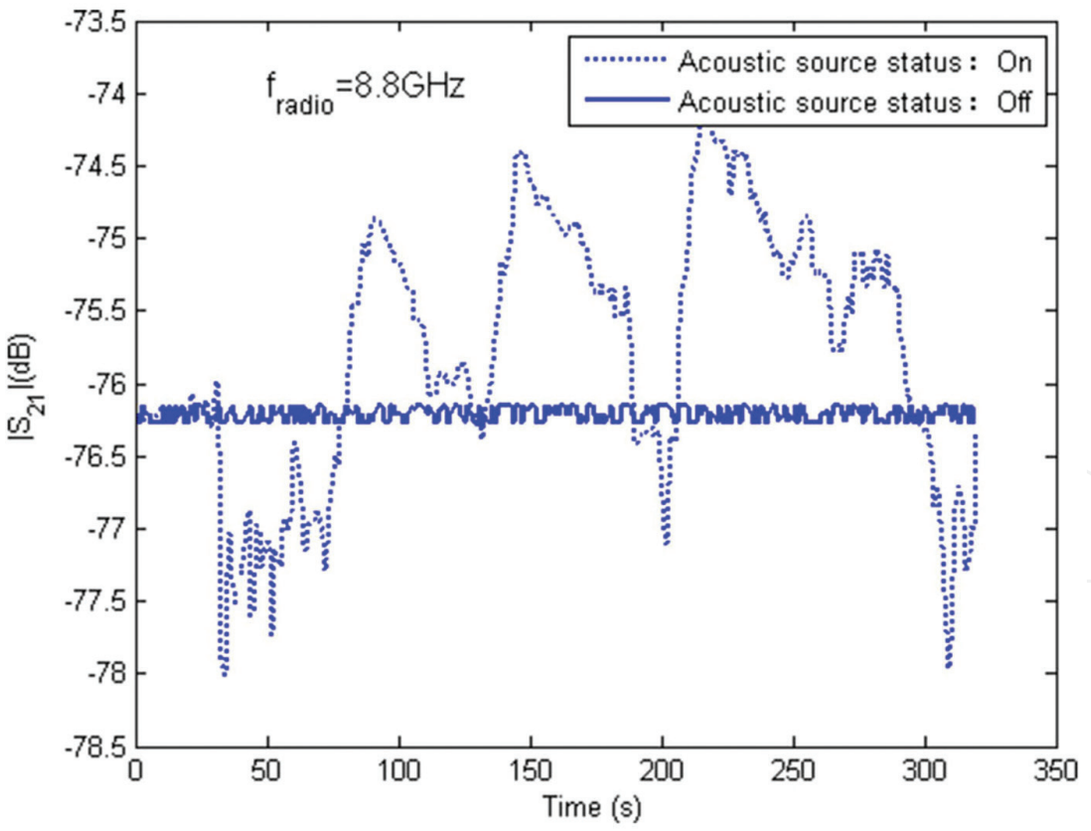

Figure 11. The testing result of 8.8 GHz stimulated by the "double-slit" acoustic source.

http://dx.doi.org/10.5772/intechopen.70996

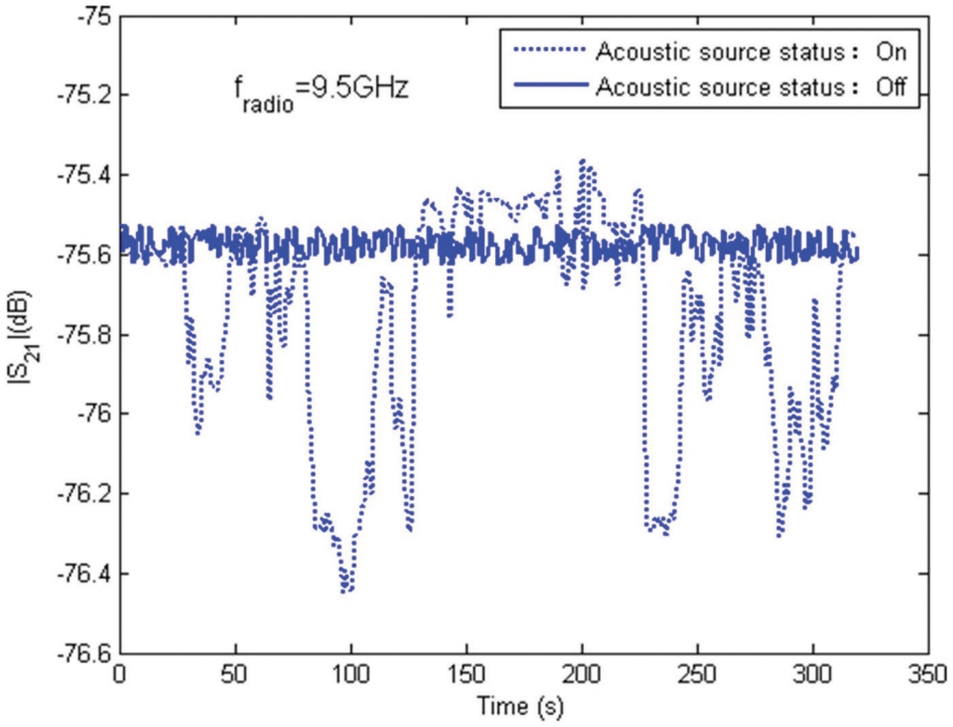

Figure 12. The testing result of 9.5 GHz stimulated by the "double-slit" acoustic source.

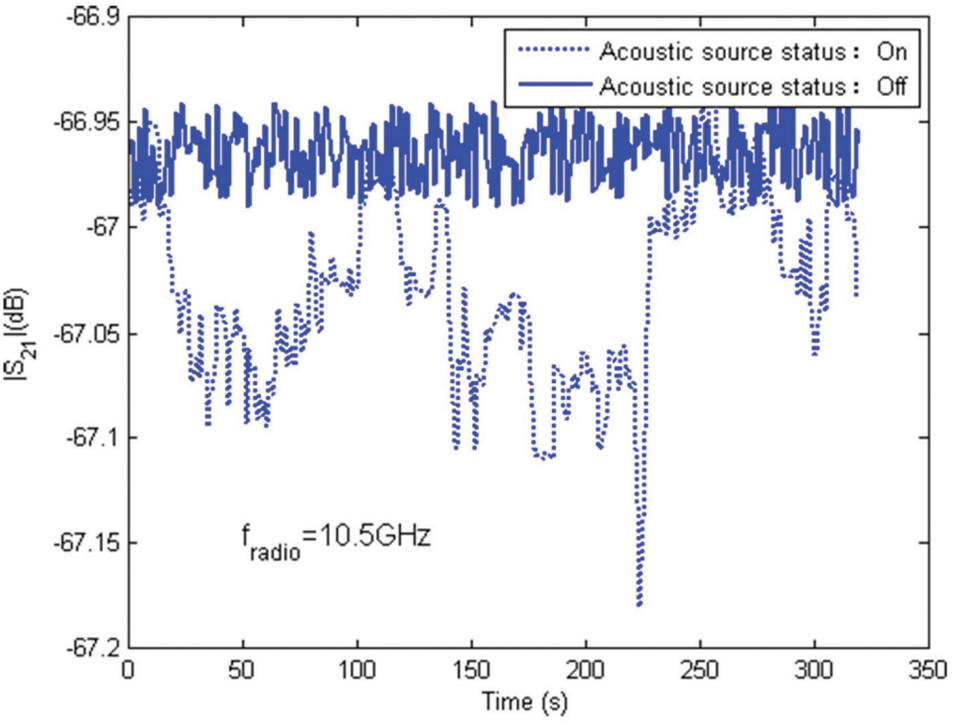

Figure 13. The testing result of 10.5 GHz stimulated by the "double-slit" acoustic source.

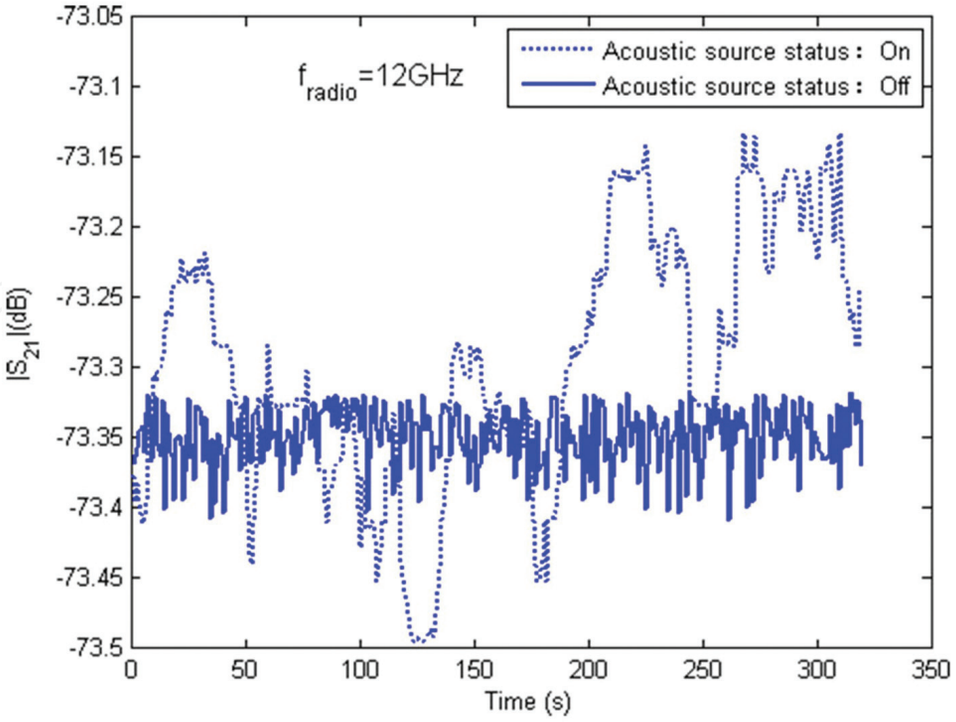

Figure 14. The testing result of 12 GHz stimulated by the "double-slit" acoustic source.

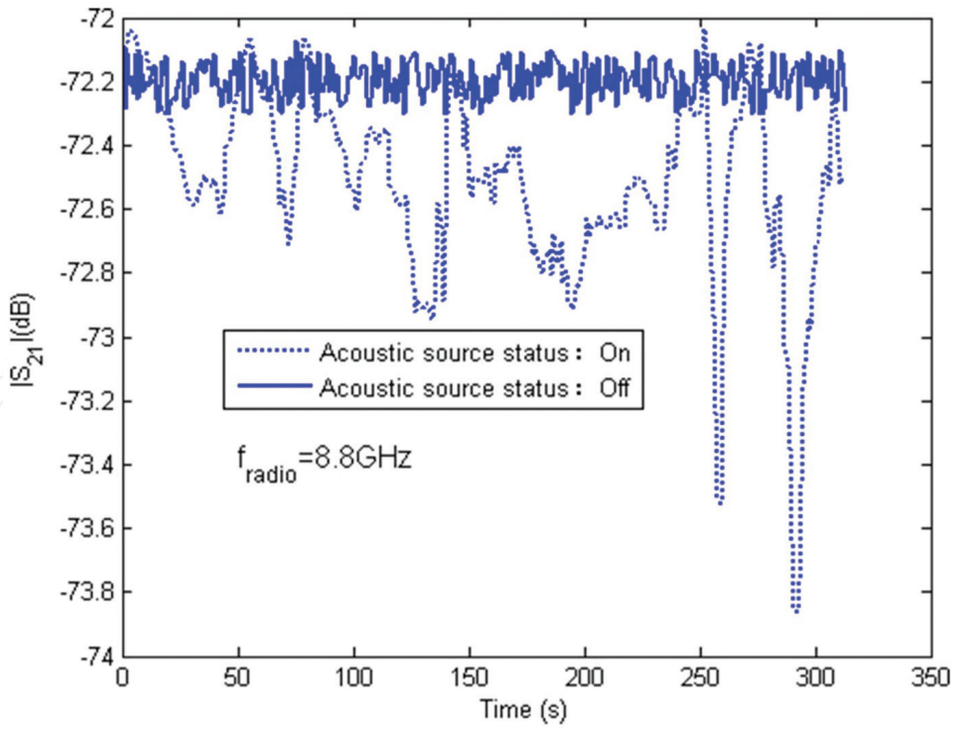

Figure 15. The testing result of 8.8 GHz stimulated by the "7 × 7 hole" acoustic source.

http://dx.doi.org/10.5772/intechopen.70996

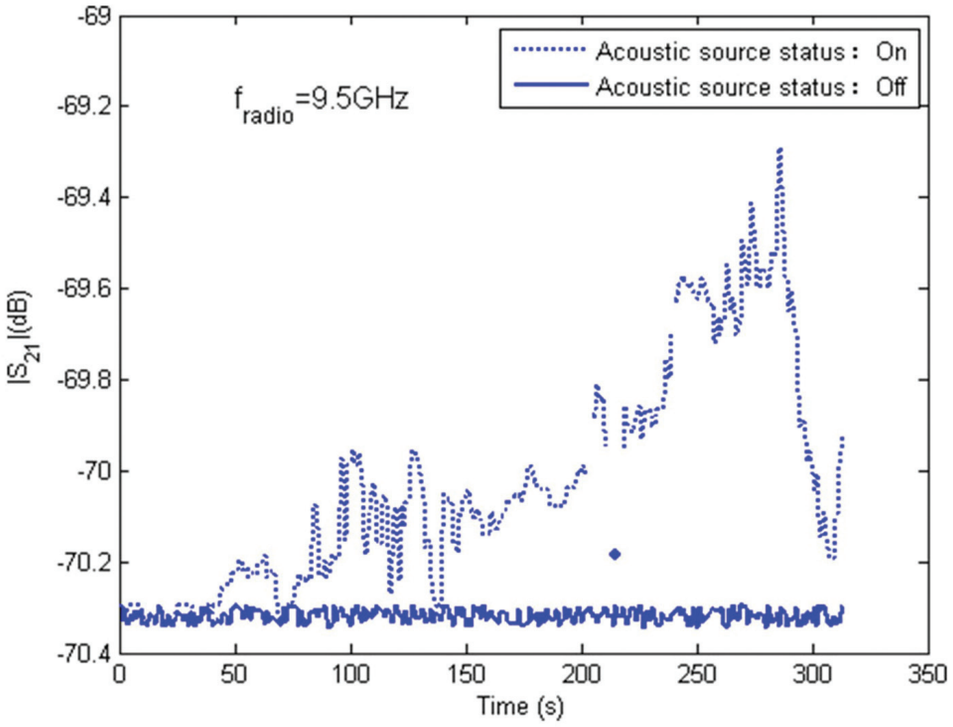

Figure 16. The testing result of 9.5 GHz stimulated by the "7 × 7 hole" acoustic source.

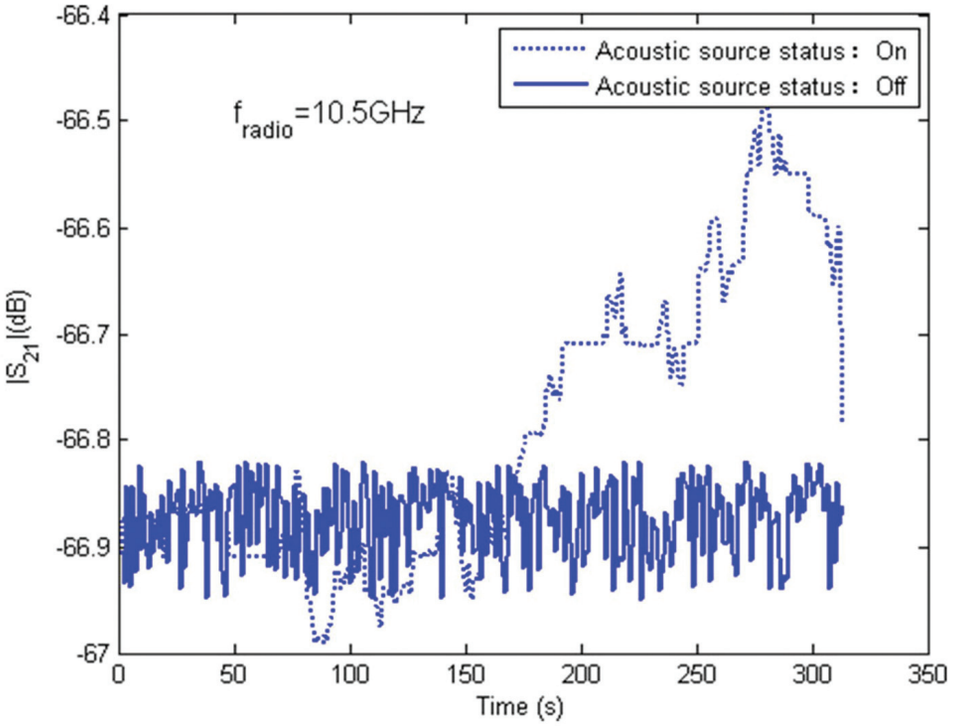

Figure 17. The testing result of 10.5 GHz stimulated by the "7 × 7 hole" acoustic source.

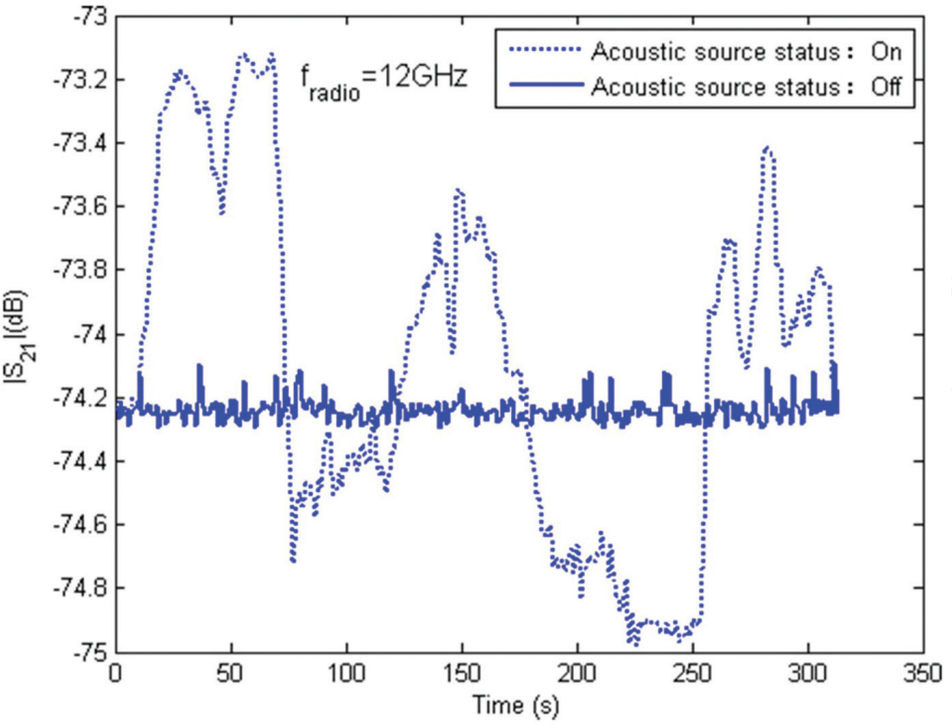

Figure 18. The testing result of 12 GHz stimulated by the "7 × 7 hole" acoustic source.

3. The interaction between a radio wave and the artificial refractivity fluctuation

According to [18], the spatial distribution of the acoustic pressure caused by the uniform spherical-surface acoustic source planar array shown in **Figure 5** is

$$p = \frac{p_A}{r - r_0} e^{-\alpha(r-r_0)} e^{j[\omega t - k(r-r_0)]} \left| S(\theta, \phi) \right| \tag{14}$$

where α denotes the attenuation coefficient of acoustic wave and $|S(\theta, \phi)|$ is the array factor of Eq. (12). The instantaneous ΔN_{C_I} and the effective ΔN_{C_E} of the atmospheric refractivity fluctuation ΔN at a space point are given by

$$\Delta N_{C\_I} = \left(77.6T^{-1} + 373265e^2T^{-2}P^{-1}\right) \cdot 10^{-2} \cdot p \tag{15}$$

$$\Delta N_{C\_E} = 0.707 \cdot \left(77.6T^{-1} + 373265e^2T^{-2}P^{-1}\right) \cdot 10^{-2} \cdot |p| \tag{16}$$

where p is the instantaneous acoustic pressure in Pa and $|p|$ denotes the amplitude of the acoustic pressure harmonically changing over time in Pa. The effective acoustic pressure can be given as $0.707|p|$.

Figures 19 and **20** show the spatial distributions of atmospheric refractivity fluctuation caused by the 49 × 49 hole acoustic source. In the calculation, the attenuation coefficient of acoustic wave α and the diameter of array element are ignored. The atmospheric pressure P is 1013.25 hPa, the

http://dx.doi.org/10.5772/intechopen.70996

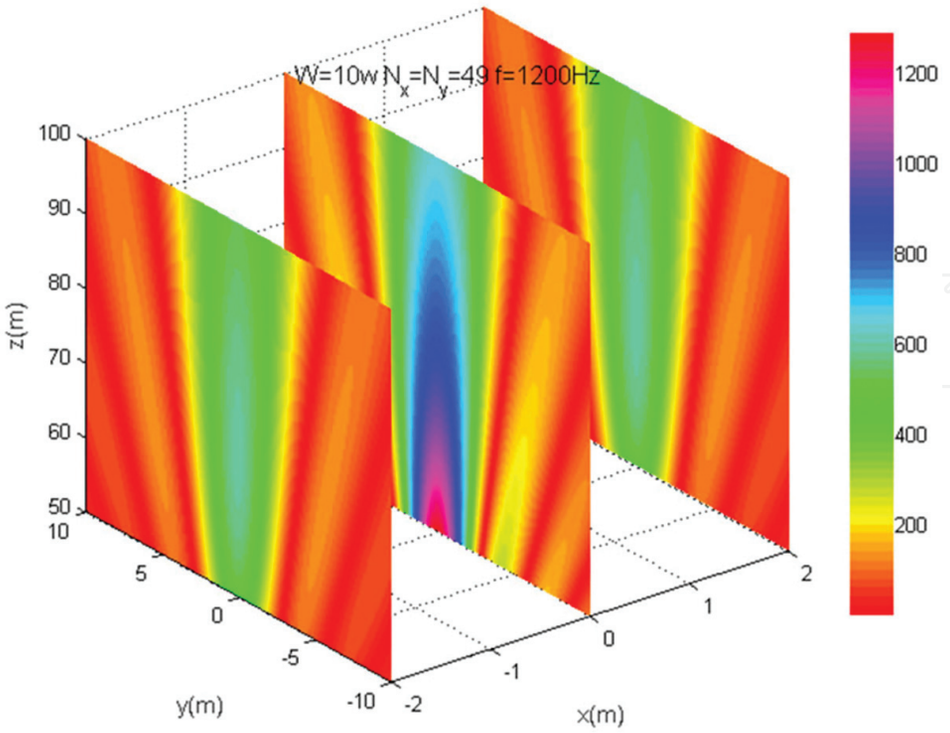

Figure 19. The spatial distribution of atmospheric refractivity parallel to the z-axis.

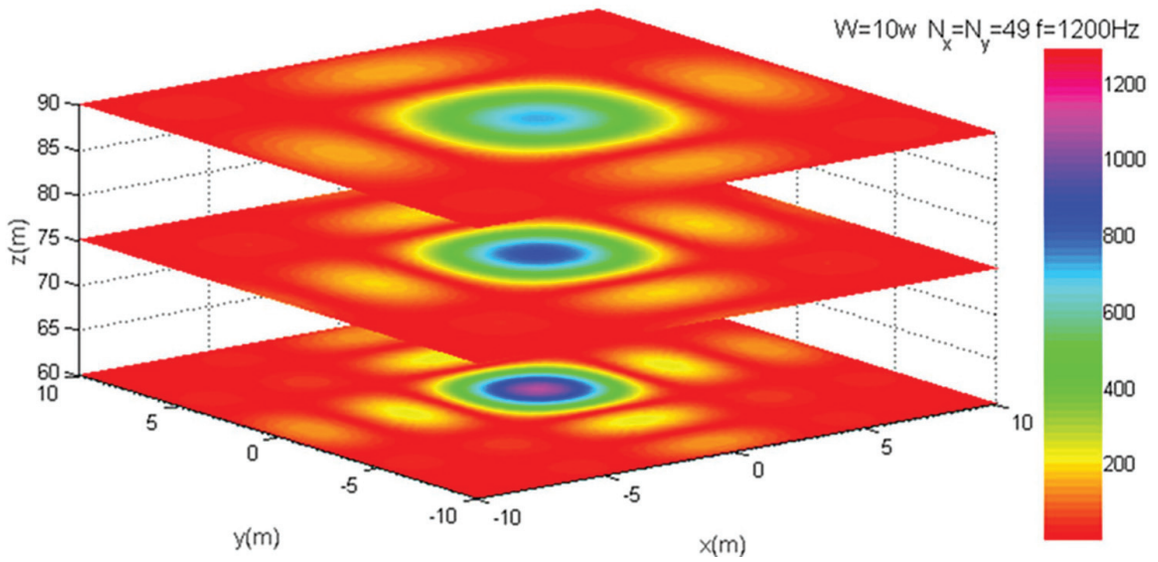

Figure 20. The spatial distribution of atmospheric refractivity parallel to the X-Y plane.

temperature T is 288.15 K, the water vapor pressure $e$is 10.02 hPa, and the power of each acoustic source element is 10 W.

As can be seen from **Figures 19** and **20**, when the coherent acoustic wave travels through the tropospheric medium, there will be a periodical atmospheric refractivity fluctuation. The

mechanism the artificial dielectric irregularities impacting the radio wave propagation is similar to that the atmospheric turbulence impacting the radio wave propagation. The atmospheric refractivity fluctuation caused by the atmospheric turbulence is stochastic distributed, and that caused by acoustic wave shows spatial periodic distribution. Therefore, the influences of atmospheric turbulence on radio wave propagation need to be analyzed by the wave propagation theory in the random medium [22], and the effects of the artificial dielectric irregularities on the radio wave propagation need to be studied using the theory of electromagnetic scattering, reflection, and refraction by the periodic structure medium. Bragg volume scattering theory and Fresnel volume scattering theory are mainly used to analyze the impacts of artificial irregularities on radio wave propagation [23–26].

Our research group is devoted to quantitatively analyzing the influences of the artificial irregularities on the amplitude, phase, propagation direction, polarization, and other parameters of an electromagnetic wave. The related exploration is possible to implement leap-forward development in the fields of electronic countermeasure, communications, radar detection, and other wireless technologies.

An experiment aims to influence Michelson interference fringes by the coherent acoustic wave-induced atmospheric refractivity fluctuation was carried out, and it qualitatively verifies the feasibility to purposefully change the phase of the electromagnetic wave by the artificial refractivity fluctuation. As shown in **Figure 21**, a light emitted by laser emits hits the beam splitter G1, which is partially reflective. One part of the light denoted by 1 is reflected, while another part of the light denoted by 2 is transmitted through G1. The path of light 1 passes through the region disturbed by the artificial refractivity fluctuation, while the light 2 travels

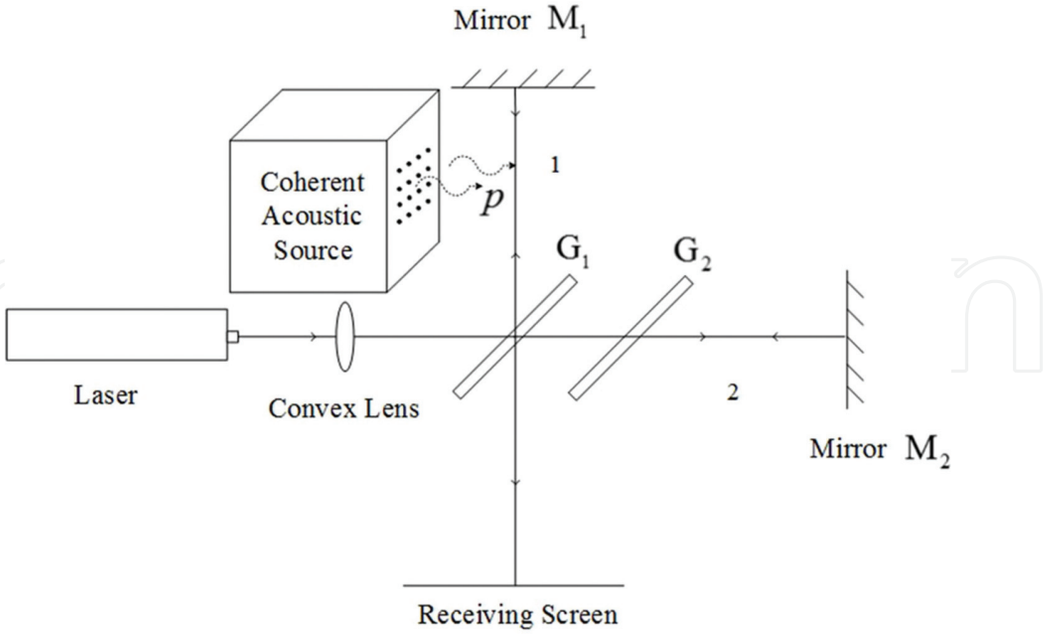

Figure 21. Artificially changing the phase of the electromagnetic wave with the help of the coherent acoustic wave-induced atmospheric refractivity fluctuation.

http://dx.doi.org/10.5772/intechopen.70996

through the normal air. Both beams meet at a receiving screen to produce an interference pattern. Comparing the interference fringes when the acoustic source is on and off, the feasibility of artificially changing the phase of the electromagnetic wave is demonstrated.

As shown in **Figure 9**, the 7 × 7 hole acoustic excitation system working at 300 Hz is adopted in the testing experiment; its parameters are shown in **Table 1**. Before the acoustic source is on, a dark fringe is in the center of the interference fringes as shown in **Figure 22**. After the acoustic source is on, the variation of the interference fringes is captured by a high-resolution vidicon. The typical frame pictures are extracted by a video processing software, which are shown in **Figures 23–26**. **Figures 23–26** obviously show that the central fringe is gradually changing. So the experimental results qualitatively verify the feasibility to purposefully change the phase of the electromagnetic wave by the artificial refractivity fluctuation.

Parameter	**Total power of the horn speaker**	**Diameter of the horn speaker**	**Diameter of the inner cavity hole**	**Diameter of the external cavity holes**
Value	5 W	0.10 m	5 mm	2 mm
Parameter	Structure	Distance between the front panels of the inner and external cavities		Interval of the external cavity holes
Value	7 × 7	1.2 m		30 mm

Table 1. The parameters of the 7 × 7 hole coherent acoustic source in **Figure 9**.

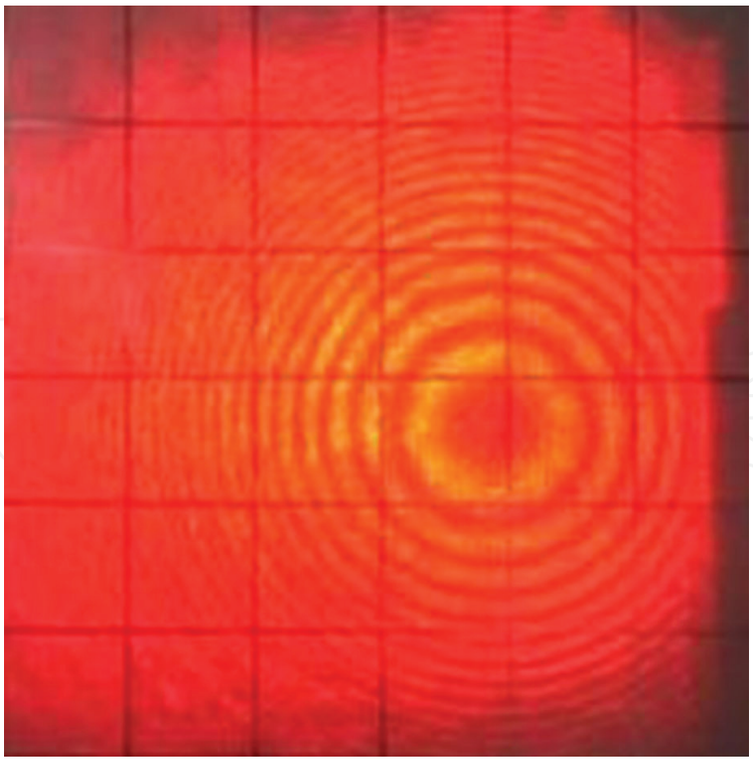

Figure 22. The fringe pattern of Michelson interferometer before the acoustic source is on.

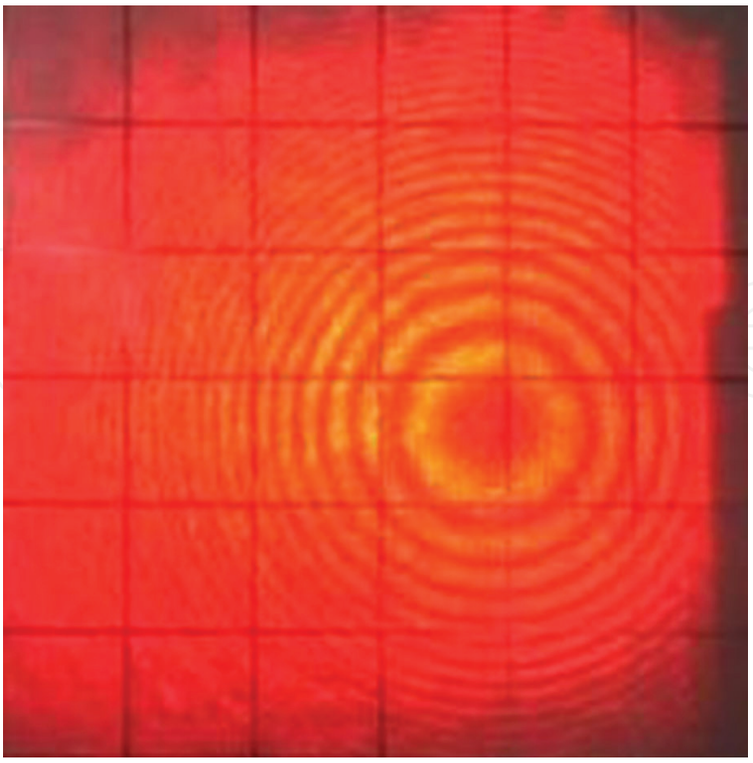

Figure 23. The fringe pattern 1 of Michelson interferometer after the acoustic source is on.

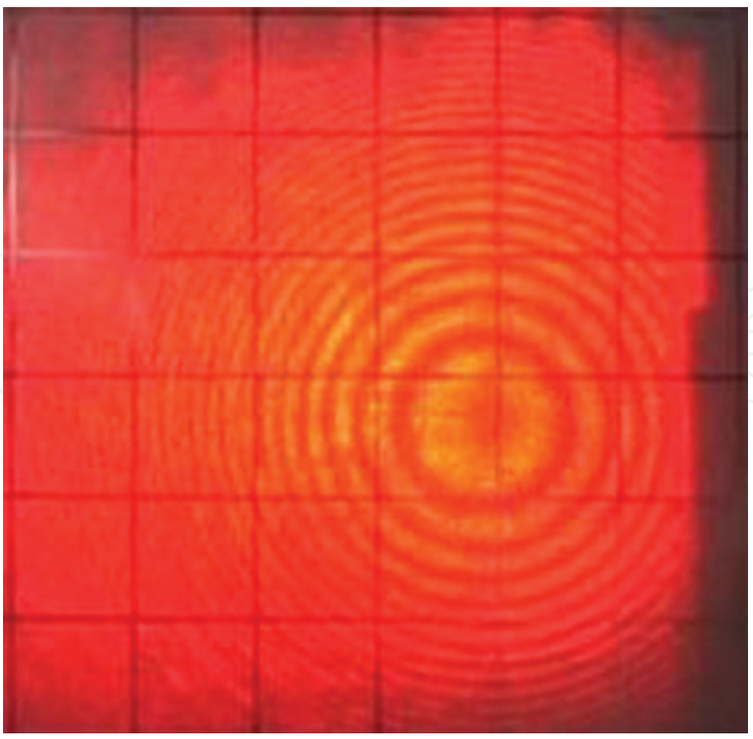

Figure 24. The fringe pattern 2 of Michelson interferometer after the acoustic source is on.

http://dx.doi.org/10.5772/intechopen.70996

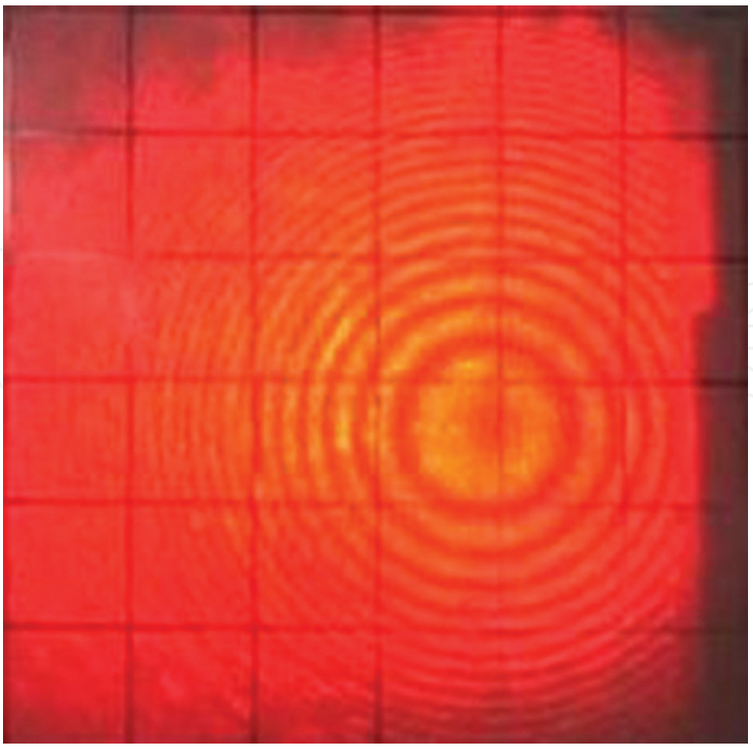

Figure 25. The fringe pattern 3 of Michelson interferometer after the acoustic source is on.

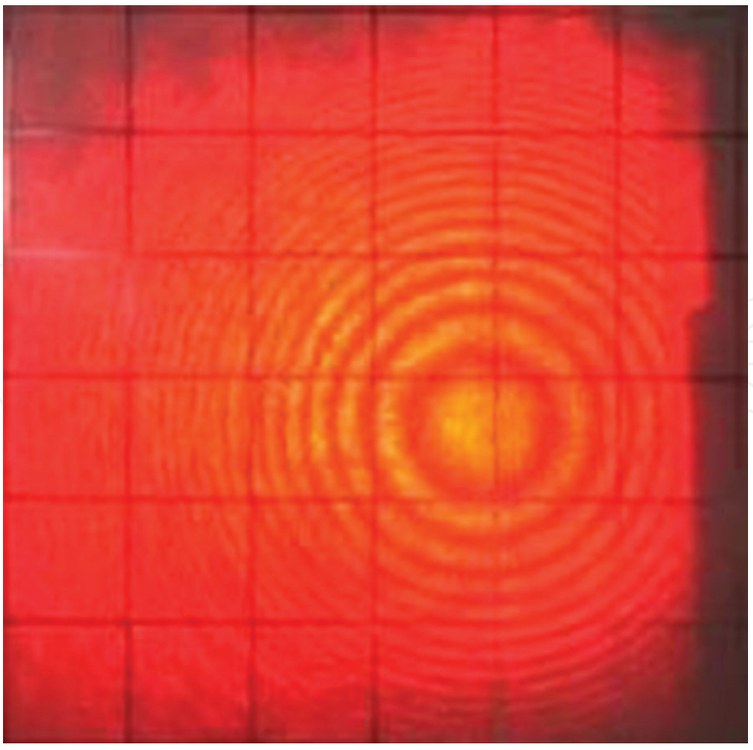

Figure 26. The fringe pattern 4 of Michelson interferometer after the acoustic source is on.

4. The potential application aspects of the artificial refractivity fluctuation

This chapter proposes a new way to purposely affect radio wave propagation by controlling and adjusting the artificial atmospheric refractivity irregularity distribution. Based on the accurate calculation of the electromagnetic wave scattering, reflection, and refraction in the areas with the artificial atmospheric refractivity irregularities, the amplitude, phase, propagation direction, polarization, and other parameters of an electromagnetic wave can be controlled artificially, so that we can purposely exert the environment media-caused positive or negative effects on radio wave propagation. The method of altering the properties of electromagnetic waves by a coherent acoustic wave-induced tropospheric refractivity fluctuation is possible to realize leap-forward development in the fields of emergency troposcatter communication, the over-the-horizon radar stealth in evaporation duct environments, electromagnetic countermeasure of coherent imaging technique, and so on. The more applications need to be explored and discovered by researchers harnessing their clever and wisdom.

The artificial dielectric irregularities are more stable and lasting than the atmospheric turbulence, and its distribution construction can be steered artificially. It is obvious that the artificial dielectric irregularities can be used to effectively improve the stability of the troposcatter communication channel. Based on the experiment shown in **Figures 23**, **24, 25**, and **26**, if the amount of phase shift caused by the coherent acoustic waves is quantitatively calculated, the interference fringes on the receiving screen can be artificially controlled. In a similar way, the artificial dielectric irregularities can be used to disturb the coherent optical imaging radar. In what follows, the mechanism of the application to the over-the-horizon radar stealth in evaporation duct environments is briefly discussed.

Because of some natural phenomena, such as the evaporation of sea water, heat exchange between air, and sea surface, as the height increases, the water vapor pressure rapidly decreases, and the temperature increases, which causes a steep fall in N. If the refractivity gradient meets the condition of $\mathrm{d}N/\mathrm{d}h < -0.157$ N-unit/m, the evaporation duct will arise in the specific region. If the wavelength of a radio wave is short enough and its angle of elevation is small enough, the super-refraction of radar wave over the sea surface will occur. In other words, the evaporation duct can be regarded as a natural waveguide which steers the radio signal from the transmitter to a receiver that may be situated well beyond the radio horizon.

If coherent acoustic sources are set around the target to be protected, the evaporation duct environment will be destroyed when the acoustic wave-induced refractivity fluctuation makes the refractivity gradient not accord with $\mathrm{d}N/\mathrm{d}h < -0.157$ N-unit/m, so that the target will not be detected by the over-the-horizon radar in evaporation duct environment. **Figure 27** shows the simulation of the refractive index profile of evaporation duct environment. **Figure 28** shows the simulation of the refractive index profile of evaporation duct when coherent acoustic waves are applied. Comparing the results in **Figures 27** and **28**, it can be concluded that the refractive index profile of evaporation duct is easily destroyed by coherent acoustic waves.

The potential applications proposed in this section based on the mechanism altering the properties of an electromagnetic wave by coherent acoustic wave-induced tropospheric refractivity

http://dx.doi.org/10.5772/intechopen.70996

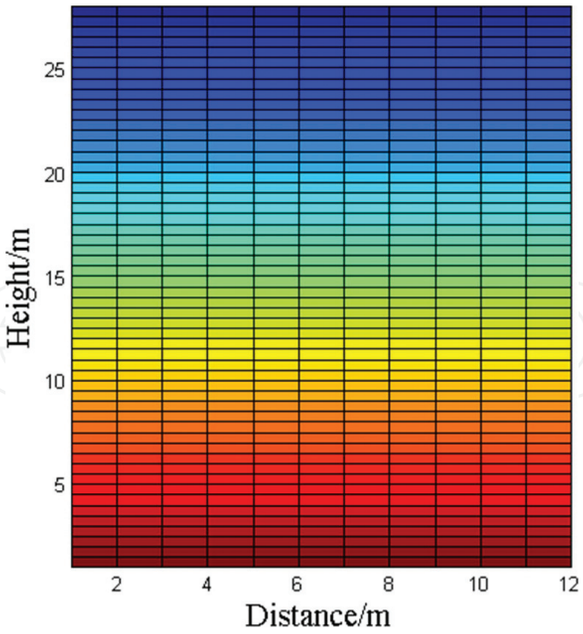

Figure 27. The refractive index profile of evaporation duct environment.

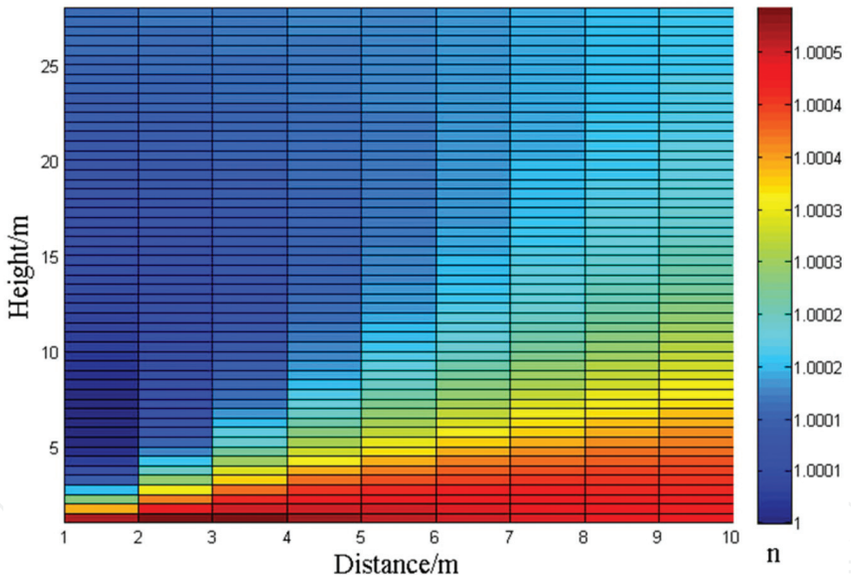

Figure 28. The refractive index profile of the disturbed evaporation duct environment.

fluctuation are still in the infant stage. There is still a long way to go for the technology development and more applications.

5. Conclusion

The idea of this chapter is logical in theory, and its feasibility is qualitatively verified in [18]. The mechanism the artificial dielectric irregularities impacting radio wave propagation is

similar to that the atmospheric turbulence impacting radio wave propagation. The Bragg volume scattering theory and Fresnel volume scattering theory provide the theoretical basis for quantitatively analyzing the influences of the artificial irregularities on the amplitude, phase, propagation direction, polarization, and other parameters of an electromagnetic wave. The experiment that effectively controlled Michelson interference fringes by the coherent acoustic waves further qualitatively verifies the feasibility of purposefully changing the phase of the electromagnetic wave by the artificial dielectric irregularities. The technique of altering the properties of an electromagnetic wave by coherent acoustic wave-induced tropospheric refractivity fluctuation is very possible to realize leap-forward development in the fields of emergency troposcatter communication and the over-the-horizon radar stealth in evaporation duct environments. However, the investigation is in its infant stage; there is still a long way to go for the technology development and more applications. In order to further investigate the point of view put forward in this chapter, the following issues need to be considered deeply: quantitatively investigating the spatial distribution of atmospheric refractivity under the interaction of coherent acoustic waves and atmospheric turbulence, determining the specific influence mode of the artificial dielectric irregularities on radio wave propagation, such as reflection, scattering, refraction, and diffraction, quantitatively calculating the physical and electromagnetic properties of the artificial dielectric irregularities, quantitatively estimating the impact degree of the artificial dielectric irregularities on radio wave propagation, and discovering more application modes of this technique.

Acknowledgements

The authors would like to thank the support of National Natural Science Foundation of China (grant no. 61771375), and they would also like to thank the teachers and students who are devoted to exploring the idea of this chapter.

Author details

Shuhong Gong[1,2]*, Yu Liu[1,2], Muyu Hou[1,2] and Lixin Guo[1,2]

*Address all correspondence to: ljbrp2003@aliyun.com

1 School of Physics and Optoelectronic Engineering, Xidian University, Xi'an, China

2 Collaborative Innovation Center of Information Sensing and Understanding, Xidian University, Xi'an, China

References

[1] Tonning A. Scattering of electromagnetic wave by an acoustic disturbance in the atmosphere. Applied Science Res. 1957;**6**(1):401-421. DOI: 10.1007/BF02920397

[2] Bhatnagar N, Peterson A. Interaction of electromagnetic and acoustic waves in a stochastic atmosphere. IEEE Transactions on Antennas and Propagation. 1979;**AP-27**:385-393. DOI: 10.1109/TAP.1979.1142091

[3] Frankel M, Chang N, Sanders M Jr. A high-frequency radio acoustic sounder for remote measurement of atmospheric winds and temperature. Bulletin American Meterological Society. 1977;**58**:928-933. DOI: 10.1175/1520-0477(1977)058<0928:AHFRAS>2.0.CO;2

[4] Marshall J, Peterson A, Barnes A Jr. Combined radar-acoustic sounding system. Applied Optics. 1972;**II**:108-112. DOI: 10.1364/AO.11.000108

[5] Max North E, Peterson AM, Dean Perry H. RASS, a remote sensing system for measuring low-level temperature profiles. Bulletin of the American Meteorological Society. 1973;**54**(9): 912-919. DOI: 10.1175/1520-0477(1973)054<0912:RARSSF>2.0.CO;2

[6] Daas M, Knochel R. Microwave-acoustic measurement system for remote temperature profiling in closed environments. In: Microwave Conference; 5-9 Sept. 1992; Helsinki, Finland. IEEE; 1992. p. 1225-1230. DOI: 10.1109/EUMA.1992.335871

[7] WeiB M, Knochel R. A Monostatic radio-acoustic sounding system. In: Microwave Symposium Digest, 1999 IEEE MTT-S International; 13-19 June 1999; Anaheim, CA, USA. IEEE. p. 1871-1874. DOI: 10.1109/MWSYM.1999.780338

[8] WeiB M, Knochel R. A Monostatic radio-acoustic sounding system used as an indoor remote temperature profiler. IEEE Trans. on Instrumentation and Measurement. 2001;**50**(5): 1043-1047. DOI: 10.1109/19.963155

[9] Brooker G, Martinez J. Low-cost Monostatic radio-acoustic sounding system for indoor temperature profiling. In: Radar Conference; 26-30 May 2008; Rome, Italy. IEEE; 2008. p. 245-250. DOI: 10.1109/RADAR.2008.4720764

[10] Saffold J, Williamson F,Ahuja K,Stein L, Muller M. Radar-acoustic interaction for IFF applications. In: Radar Conference; 22-22 April 1999; Waltham, MA, USA. USA: IEEE; 1999. p. 198-202. DOI: 10.1109/NRC.1999.767313

[11] Hanson J, Marcotte F. Aircraft wake vortex generation using continuous-wave radar. Technical Digest. 1997;**18**:348-357

[12] Marshall RE, Myers TJ. Wingtip generated wake vortices as radar targets. In: Radar Conference; 13-16 May 1996; Ann Arbor, MI, USA. IEEE; 1996. p. 184-189. DOI: 10.1109/NRC.1996.510678

[13] Alexander SP. Studies of the Lower Troposphere [thesis]. Adelaide, Australia: University of Adelaide; 2004. p. 34

[14] Peters G. History of RASS and its use for turbulence measurements. In: Geoscience and Remote Sensing Symposium, 2000. Proceedings. IGARSS 2000. IEEE 2000 International; 24-28 July 2000; Honolulu, HI, USA. USA: IEEE; 2000. p. 1183-1185. DOI: 10.1109/IGARSS.2000.858061

[15] Angevine WM. Radio acoustic sounding system (RASS) applications and limitations. In: Geoscience and Remote Sensing Symposium; 24-28 July 2000; Honolulu, HI, USA. USA: IEEE; 2000. p. 1180-1182. DOI: 10.1109/IGARSS.2000.858060

[16] Ulyanov YN, Maksimova NG, Misaylov VL. Radioacoustic sounding with the use of wideband acoustic impulses. In: Ultrawideband and Ultrashort Impulse Signals; 15-19 Sept. 2008; Sevastopol, Crimea, Ukraine: IEEE; 2008. p. 249-251. DOI: 10.1109/UWBUS.2008.4669425

[17] Furumoto J-i, Shinoda T, Tsuda T. Continuous monitoring of temperature profiles with a excellent vertical resolution by applying frequency domain Interferometric imaging technique to the radio acoustic sounding system with a wind profiling radar. In: ICROS-SICE International Joint Conference; 18-21 Aug. 2009; Fukuoka, Japan: IEEE; 2009. p. 1312-1315

[18] Gong S, Yan D, Wang X. A novel idea of purposefully affecting radio wave propagation by coherent acoustic Source-induced atmospheric refractivity Fluctuation. Radio Science. 2015;**50**(10):983-996. DOI: 10.1002/2015RS005660

[19] Hall MPM. Atmospheric Refractivity, in Tropospheric Propagation and Radio Communication. translated by Z. Liang, and Z. Zhang. Beijing:1984

[20] Gong S. Study on some Problems for Radio Wave Propagating and Scattering through Troposphere [Thesis]. Xi'an, China: Xidian University; 2008

[21] Du G, Zhu Z, Gong X. Basic Properties of Acoustics, in Basic of Acoustics. Shanghai, China: Shanghai Sci. and Technol; 1991

[22] Ishimaru A. Wave Propagation and Scattering in Random Medium. NewYork, NY, USA: Academic press; 1978

[23] Kallistratova MA. Backscattering and reflection of acoustic waves in the stable atmospheric boundary layer. In: 14th International Symposium for the Advancement of Boundary Layer Remote Sensing; IOP Conf.Series:Earth and Environmental Science; 2008. DOI: 10.1088/1755-1307/1/1/012001

[24] Kirkwood S, Belova E, Satheesan K, Narayana Rao T, Rajendra Prasad T, Satheesh Kumar S. Fresnel scatter revisited – Comparison of 50MHz radar and Radiosondes in the Arctic. The Tropics and Antarctica. 2010;**28**:1993-2005. DOI: 10.5194/angeo-28-1993-2010

[25] Jagdhuber T. An approach to extended Fresnel scattering for modeling of depolarizing soil-trunk double-bounce scattering. Remote Sensing. 2016;**8**:818. DOI: 10.3390/rs8100818

[26] Gage KS, Balsley BB, Green JL. Fresnel scattering model for specular echoes by VHF radar. Radio Science. 1981;**16**(6):1447-1453. DOI: 10.1029/RS016i006p01447